

Potential of Biomimetic Apatite Precipitation Induced by Polydopamine Nanolayers for Design of Biointerfaces

Seyed Mohsen Latifi¹, Ravi Shankar², Henry J. Donahue*

^{1,2,*}Bone Engineering Science and Technology (BEST) Lab, Department of Biomedical Engineering, Virginia Commonwealth University, Richmond, Virginia, USA

Abstract

Nanolayers of polydopamine (PDA) have potential to facilitate mineralization of apatite in the presence of simulated body fluid. The aim of this work was to determine the parameters that affect biomimetic apatite precipitation induced by a PDA nanolayer. For this purpose, a PDA nanolayer was created on different substrates. The effect of four parameters; substrate orientation, volume of simulated body fluid, and substrate material; on apatite precipitation in 1.5×simulated body fluid was evaluated by scanning electron microscope. Results showed that apatite precipitation on PDA coated samples was substrate independent; but was highly affected by substrate orientation and volume of simulated body fluid. Additionally, substrate orientation affected the size of precipitated apatite ranging from nano (less than 100 nm) to micron size (~4.3 μm). This information can be used to design biomimetic biointerfaces with optimized surface properties.

Keywords: Polydopamine, Apatite, Simulated body fluid, Biointerface

1. INTRODUCTION

Biointerface design of bone graft substitutes has a strong potential to affect cellular response to grafts and consequently the osteogenic potential of the graft [1]. For example, topography is a biointerface property which can affect cell response in the bone regeneration process [2]. Therefore, it is of great interest to develop techniques which have potential to manipulate surface properties.

For bone regeneration, a desirable property of the biointerface is the ability to facilitate mineralization. Interestingly, it has been demonstrated that polydopamine (PDA) nanolayers have the potential to accelerate mineralization of apatite in 1.5×simulated body fluid (1.5×SBF). This is likely due to the abundant exposed catecholamine moieties on PDA surfaces [3-4]. However, the properties which examine mineralization on PDA are not entirely known. Therefore, in this study we examined the parameters that affect biomimetic apatite precipitation induced by a polydopamine nanolayer. This information can be used to design biomimetic biointerfaces with optimized surfaces to facilitate mineralization.

2. MATERIALS AND METHODS

2.1 Substrates preparation

Three types of material were used as substrates in this study. These included commercially pure titanium (Ti, 20mm x 10mm x 2mm) and borosilicate glass coverslips (d = 22mm, Fisher) plus or minus a coating of poly (ε-caprolactone) (PCL). Ti substrates were polished to nano-scale roughness by polishing for 10 min each with 220 and then 600 grit SiC paper. The substrates were then exposed to a 3μm polycrystalline diamonds suspension (Buehler) and polished with a Microcloth (Buehler). This was repeated with a 0.06μm colloidal silica suspension with another Microcloth. Ti substrates were then ultrasonically degreased by placement, two times, in acetone for 30 min. Slides were placed in isopropanol for 30 min and deionized water for 30 min.

2.2 Experimental procedures

For this study we completed three experiments. In the first experiment, we examined the effect of substrate orientation on apatite precipitation. Ti was used as a substrate as its biocompatibility and mechanical properties make it a common component of bone implants. Nanorough Ti samples were PDA coated and placed into one of three 50 mL tubes, with one positioned vertically (V sample), one with the PDA coated side up (U sample), and one with the PDA coated side facing down (D sample). To create a PDA nanolayer on substrates, the substrates were incubated for 24 h at 37 °C in a dopamine-hydrochloride solution in 10 mM tris buffer, pH adjusted to 8.5 [5]. Substrates were then rinsed thoroughly in deionized water. The tubes were filled with 45 ml 1.5×simulated body fluid (1.5× SBF) and incubated at 37 °C for 3 days, replacing the 1.5×SBF every day, to precipitate apatite. The substrates were then rinsed with deionized water, and air dried for 24 h at 37 °C. 1.5×SBF with ion

concentrations (Na^+ , 213; K^+ , 7.5; Mg^{2+} , 2.25; Ca^{2+} , 3.75; Cl^- , 221.7; HCO_3^- , 6.3; HPO_4^{2-} , 1.5 and SO_4^{2-} , 0.75 mM) 1.5 times that of SBF was prepared according to the protocol described by Kokubo and Takadama [6].

In the second experiment we examined the effect of 1.5×SBF on apatite precipitation. Nanorough Ti samples, similar to those used in the first experiment, were coated with PDA and placed in two 50 mL tubes and incubated at 37 °C for 2 days, in either 25 mL or 45 mL 1.5×SBF replaced every day.

In the third experiment we examined the effect of substrate material on apatite precipitation. Three different materials, including metal (Ti polished to nano-scale roughness), uncoated glass (borosilicate coverslip), and polymer (PCL) coated glass underwent the same apatite precipitation process as above. Substrates were PDA coated and then incubated in 1.5×SBF at 37 °C for 1 day.

2.3 Characterization

Samples from each of the three experiments were platinum sputter coated before imaging with a scanning electron microscope (Hitachi FE SEM Su-70). Image J analysis was performed on the SEM images to determine the size and the surface coverage of precipitated apatite. Energy dispersive X-ray spectrometer (EDX) was used to identify the chemical composition of the precipitated apatite. The roughness of the substrates was assessed by atomic force microscopy (Bruker Bioscope AFM). Static contact angle of water droplets on the substrates was quantified with a contact angle goniometer, using 5 µl of distilled water.

2.4 Statistical analysis

Quantitative data is expressed as means ± standard deviation. Statistical comparisons were carried out using a t-test or a one-way ANOVA followed by Tukey’s post-hoc test. P values <0.05 indicated a significant difference.

3. RESULTS AND DISCUSSION

To create a PDA nanolayer on substrates, substrates were incubated for 24 h at 37 °C in a dopamine-hydrochloride solution. Fig. 1 shows the effect of substrate (nanorough Ti) orientation on apatite precipitation after 3 days incubation in 1.5×SBF (replaced each day) at 37 °C.

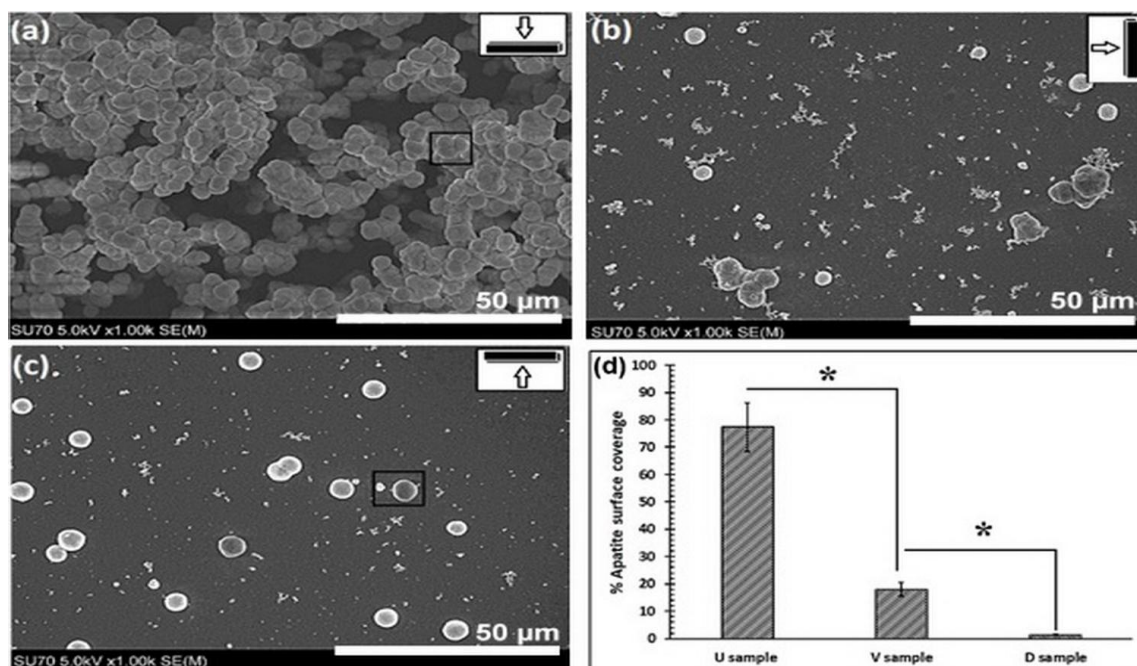


Fig. 1: SEM images of precipitated apatite on nanorough Ti substrates with different orientations after 3 days incubation in 1.5×SBF at 37 °C; (a) U sample, (b) V sample, and (c) D sample. (d) Percentage of apatite surface coverage for different substrate orientations (n=5, *p<0.05). Substrate orientation is depicted in the upper right hand corner of each image.

Substrate orientation affected the size and amount of precipitated apatite. The U sample (Fig. 1a) had uniform micron particles and a greater level of apatite precipitation (77.39 ± 8.92 % apatite surface coverage) than either the V sample (Fig. 1b) or the D sample (Fig. 1c). The V sample had more apatite precipitation (17.91 ± 2.50 % apatite surface coverage) than the D sample (1.33 ± 0.29 % apatite surface coverage). Additionally, the V sample had more micro- and nano-scale features than the D sample. Data from the U sample suggest that the direction of the gravity vector acts as a driving force for the capture of ions by the PDA layer and subsequent precipitation of apatite from solution (nucleation and growth of apatite). In other words, the U sample was positioned to capture the downward ion flux, thus increasing the rate and degree of precipitation drastically over the V and D sample (Fig. 1d).

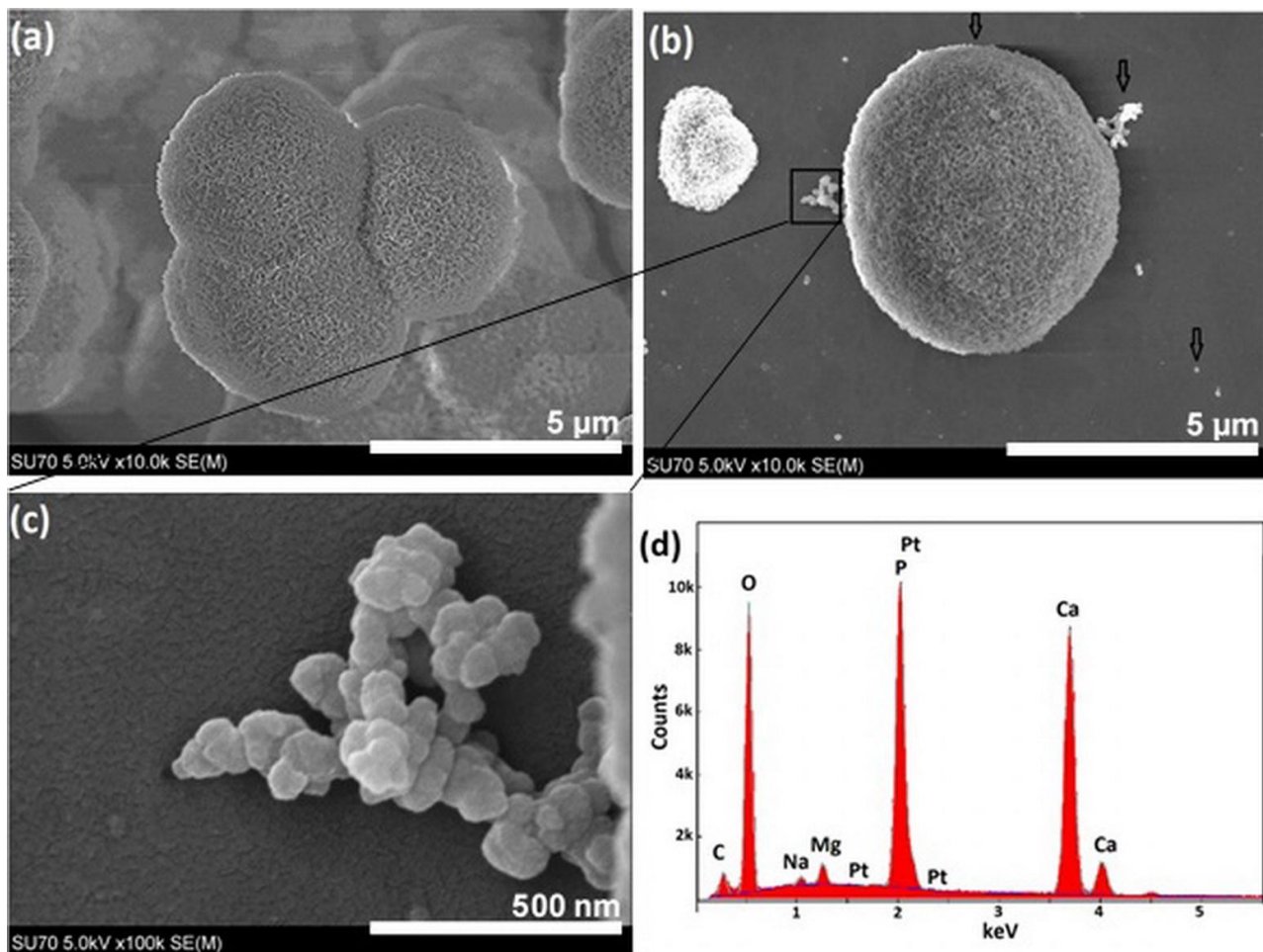


Fig. 2: High magnification of the highlighted areas in Fig.1 for (a) U sample, (b) and (c) D sample. (d) EDX spectrum of the precipitated apatite on the U sample represented in Fig. 2a.

Fig. 2 shows high magnifications ($\times 10k$ and $\times 100k$) of the highlighted areas in Fig.1 for U (Fig. 2a) and D (Fig. 2b, c) samples. Precipitated apatite on the U sample (Fig. 2a) is an agglomeration of micron spherical particles ($\sim 4.3 \mu m$) with nanorough surface features. Precipitated apatite on the D sample (Fig. 2b and c), which spread across the substrate surface, is of differing sizes including round single nanocrystals ($\sim 50nm$), irregular nanoscale agglomerations of nanocrystals ($400 - 600 nm$), and micron spherical particles ($\sim 4.3 \mu m$) with nanorough surface features. Fig. 2d shows the chemical composition of the precipitated apatite on the U sample (Fig. 2a). EDX reveals that not only Ca, P, and O, but also Mg and Na were detected in the precipitated apatite. This suggests minor incorporation of Mg and Na ions into the structure of precipitated apatite, similar to the precipitated apatite within bone mineral [7]. The presence of Pt in Fig. 2d is the result of platinum coating of samples before imaging with a SEM.

Fig. 3 shows the effect of $1.5 \times SBF$ volume on apatite precipitation on the surface of PDA coated nanorough Ti substrates (U sample) after 2 days incubation in $1.5 \times SBF$ at $37^\circ C$. The volume of $1.5 \times SBF$ above the substrate significantly affected surface apatite deposition. Substrates covered with 45ml $1.5 \times SBF$ displayed increased apatite deposition ($24.02 \pm 0.37\%$ surface

coverage) compared to substrates covered with 25 mL 1.5×SBF ($12.02 \pm 0.79\%$ surface coverage). This was likely the result of greater ion availability for apatite nucleation and growth on the surface due to the greater volume of 1.5×SBF.

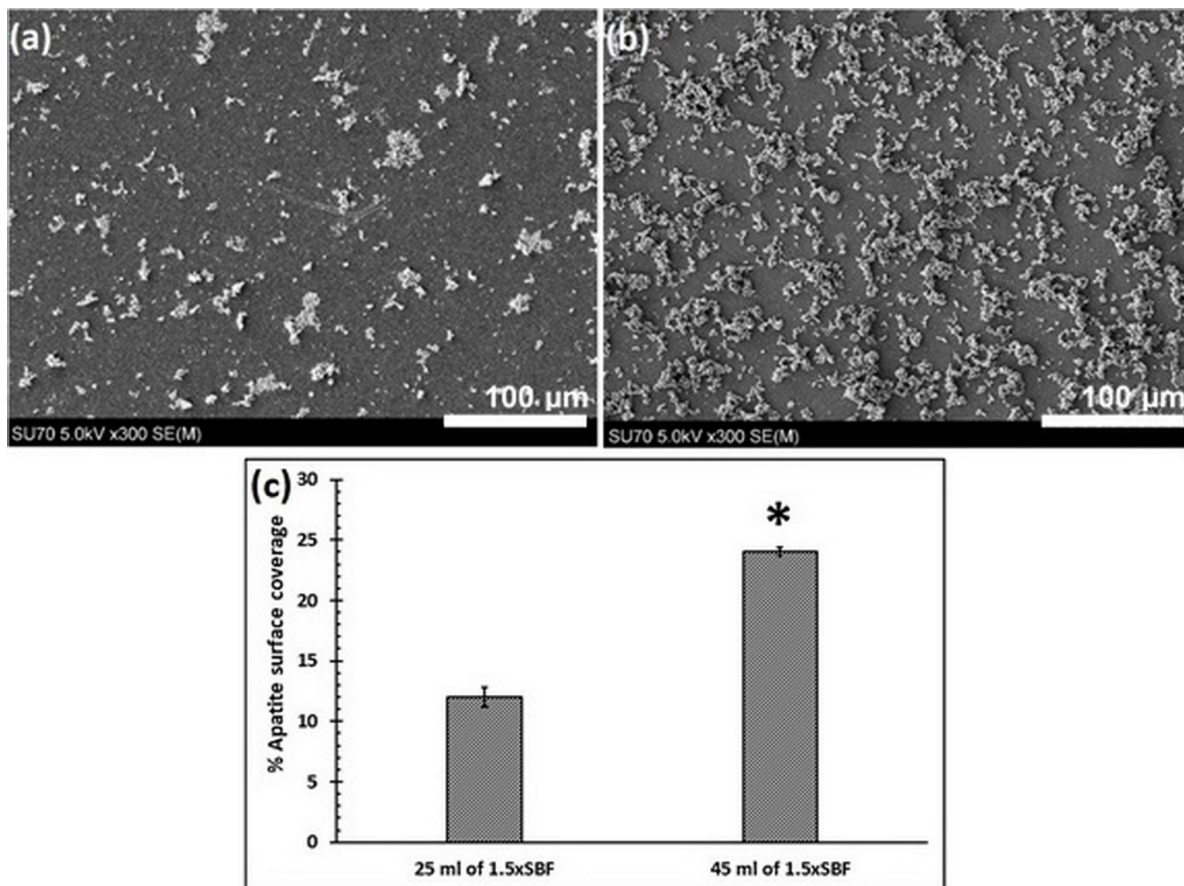


Fig. 3: SEM images of precipitated apatite on nanorough Ti (U sample) after 2 days incubation in 1.5×SBF at 37 °C while replacing the 1.5×SBF every day; (a) 25mL of 1.5×SBF, (b) 45mL of 1.5×SBF, (c) Percentage of apatite surface coverage (n=5, *p<0.05)

Table 1 shows the surface properties of three different substrates (nanorough Ti, borosilicate glass, PCL coated borosilicate glass), which is indicative of different surface chemistries, before PDA coating.

Table 1: Contact angle and roughness of different Substrates before PDA coating (n=5, *p<0.05)

properties	Nanorough Ti	Glass	PCL coated glass
Contact angle	61.97±8.08	41.38±2.57 *	62.82±2.60
Roughness (Ra)	7.17±1.64	1.69±0.65 *	8.74±1.75

Fig. 4 shows SEM images of different substrates (nanorough Ti, borosilicate glass, PCL coated borosilicate glass) prepared using the same apatite precipitation process (immersion in PDA solution for 24 h then 1.5×SBF for 1 day). As can be seen in Fig. 4, all U samples displayed similar patterns of dispersed agglomerations of apatite ranging from nano (~300 nm) to micron (~2.5 μm) size at this magnification, suggesting apatite precipitation on PDA coated samples is substrate surface chemistry-independent. In other words, only the PDA layer is sensed at the interface due to mask the substrate’s chemical signal, as detected by X-ray photoelectron spectroscopy (XPS) [5]. Moreover, results in Table 1 and Fig. 4, suggest that PDA-induced changes in surface chemistry have a greater effect on apatite precipitation than do the physical surface properties of substrate such as roughness [8].

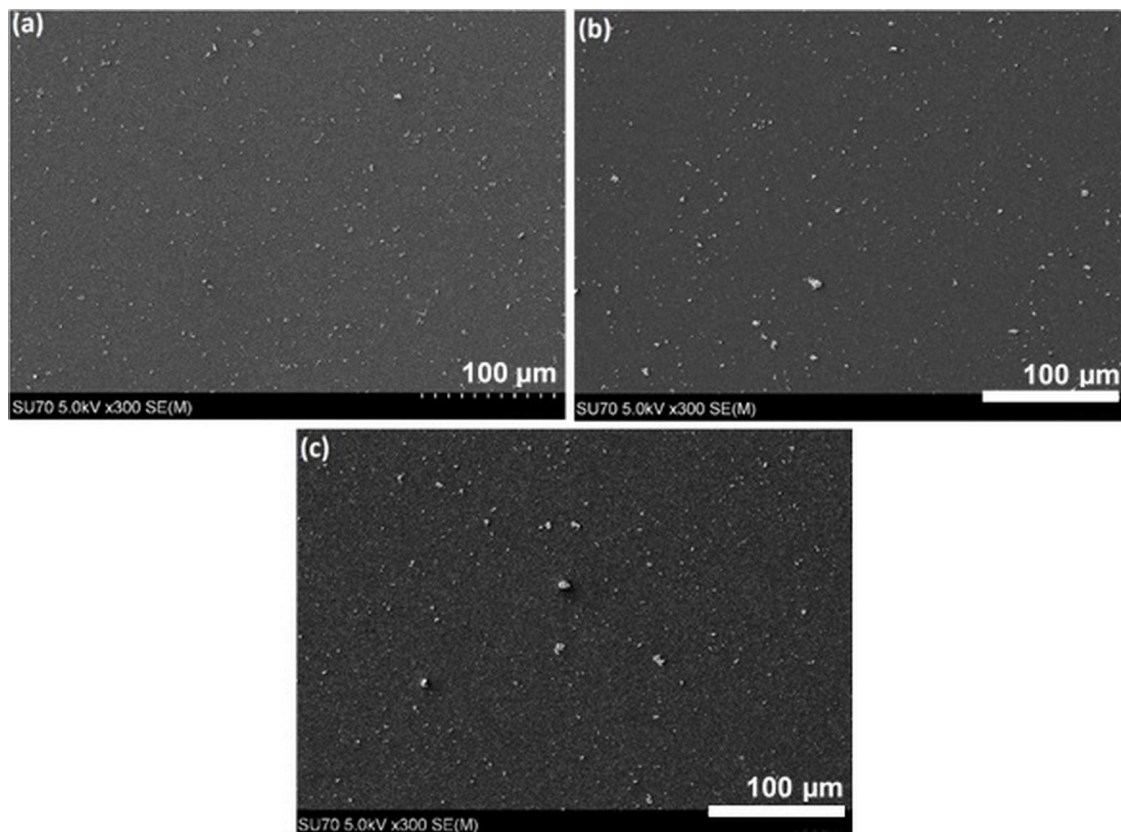


Fig. 4: SEM images of precipitated apatite on different PDA coated substrates (U samples) after 1 days incubation in 1.5×SBF at 37 °C; (a) glass, (b) PCL coated glass, (c) nanorough Ti

Previous reports suggest that the PDA nanolayer have to reach a minimum thickness to induce apatite precipitation [4] and hydrophilicity of a substrate can affect the thickness of PDA layer on the substrate [9]. Thus, hydrophilicity may have affected PDA layer thickness in our study. However, despite the different hydrophilicity of substrates we examined (Table1), the time (24h) for PDA coating process was sufficient to result in a PDA layer of sufficient thickness to facilitate apatite precipitation for all substrates we examined.

4. CONCLUSION

Our results demonstrate that apatite precipitation induced by PDA nanolayer is independent of substrate surface chemistry. However, the position of PDA coated samples and the volume of 1.5×SBF has a significant effect on the precipitation of apatite. Thus, these two parameters, especially positioning, can serve as a simple and low-cost technique for manipulating biomaterial surface characteristics such as topography.

ACKNOWLEDGEMENTS

This work is funded in part by VCU College of Engineering Foundation Research Endowment.

REFERENCES

- [1] G. Hannink, J.J. Chris Arts, "Bioresorbability, porosity and mechanical strength of bone substitutes: What is optimal for bone regeneration?" *Injury, Int. J. Care Injured*, vol. 42, 2011, pp. S22-S25. doi:10.1016/j.injury.2011.06.008
- [2] A.E. Loisel, L. Wei, M. Faryad, E.M. Paul, G.S. Lewis, J. Gao, A. Lakhtakia, H.J. Donahue, "Specific biomimetic hydroxyapatite nanotopographies enhance osteoblastic differentiation and bone graft osteointegration" *Tissue. Eng. Part A*, vol. 9, 2013, pp.1704-1712.
- [3] Z. Wang, C. Dong, S. Yang, D. Zhang, K. Xiao, X. Li, "Facile incorporation of hydroxyapatite onto an anodized Ti surface viaa mussel inspired polydopamine coating" *Appl. Surf. Sci.*, vol. 378, 2016, pp.496-503.

- [4] J. Ryu, S.H. Ku, H. Lee, C.B. Park, "Mussel-inspired polydopamine coating as a universal route to hydroxyapatite crystallization" *Adv. Funct. Mater.*, vol. 20, 2010, pp. 2132-2139.
- [5] H. Lee, S.M. Dellatore, W.M. Miller, P.B. Messersmith, "Mussel-Inspired Surface Chemistry for Multifunctional Coatings" *Science*. vol. 318(5849), 2007, pp. 426-430.
- [6] T. Kokubo, H. Takadama, "How useful is SBF in predicting in vivo bone bioactivity?" *Biomaterials*, vol. 27, 2006, pp. 2907-2915.
- [7] T. Kokubo, H.M. Kim, M. Kawashita, "Novel bioactive materials with different mechanical properties" *Biomaterials* vol. 24, 2003, pp. 2161-2175.
- [8] X. Chen, A. Nouri, Y. Li, J. Lin, P.D. Hodgson, C. Wen, "Effect of surface roughness of Ti, Zr, and TiZr on apatite precipitation from simulated body fluid" *Biotechnol. Bioeng.* vol. 101(2), 2008, pp. 378-387.
- [9] S.K. Madhurakkat Perikamana, J. Lee, Y. B. Lee, Y. M. Shin, E. J. Lee, A. G. Mikos, H. Shin, "Materials from mussel-inspired chemistry for cell and tissue engineering applications" *Biomacromolecules*. vol. 16(9), 2015, pp. 2541-2555